



Article

Gait Kinematics of Individuals with SYNGAP1-Related Disorder Compared with Age-Matched Neurotypical Individuals

Charles S. Layne ^{1,2,*}, Dacia Martinez Diaz ^{1,2}, Christopher A. Malaya ^{1,3}, Bernhard Suter ^{4,5} and Jimmy Lloyd Holder, Jr. ^{5,6,*}

- Center for Neuromotor and Biomechanics Research, Houston, TX 77204, USA; dmart205@central.uh.edu (D.M.D.); cmalaya@parker.edu (C.A.M.)
- Department of Health and Human Performance, University of Houston, Houston, TX 77204, USA
- ³ Grail Laboratory, Parker University, Dallas, TX 75229, USA
- Blue Bird Circle Rett Center, Texas Children's Hospital, Houston, TX 77030, USA; suter@bcm.edu
- Departments of Pediatrics and Neurology, Baylor College of Medicine, Houston, TX 77030, USA
- ⁶ Jan and Dan Duncan Neurological Research Institute, Texas Children's Hospital, Houston, TX 77030, USA
- * Correspondence: clayne2@uh.edu (C.S.L.); holder@bcm.edu (J.L.H.J.)

Abstract

SYNGAP1-related disorder is a rare neurodevelopmental disorder characterized by intellectual and motor disabilities, including disordered gait control. Currently, there have been few studies that have assessed the gait of individuals with SYNGAP1-related disorder using technology-based collection techniques. The purpose of this investigation was to characterize the kinematic gait pattern of these individuals using camera-based motion capture technology during treadmill walking. Both linear and non-linear analysis techniques were used to analyze bilateral lower-limb joint motion and compare the results to agematched neurotypical individuals. Results indicate that joint range of motion and velocity were decreased in the patient population relative to the neurotypical participants with the non-linear measures of angle—angle and phase portrait areas reflecting similar outcomes. The combination of linear and non-linear measures provide complementary information that, when used in combination, can provide deeper insights into the coordination and control of gait than if either of the measurement techniques are used in isolation. Such information can be useful to clinicians and therapists to develop targeted interventions designed to improve the gait of individuals with SYNGAP1-related disorder.

Keywords: gait; time-series; non-linear analysis; kinematics; SYNGAP1



Academic Editors: Juan Pedro Fuentes García and Ruperto Menayo Antúnez

Received: 5 June 2025 Revised: 17 July 2025 Accepted: 21 July 2025 Published: 25 July 2025

Citation: Layne, C.S.; Diaz, D.M.; Malaya, C.A.; Suter, B.; Holder, J.L., Jr. Gait Kinematics of Individuals with SYNGAP1-Related Disorder Compared with Age-Matched Neurotypical Individuals. Appl. Sci. 2025, 15, 8267. https://doi.org/ 10.3390/app15158267

Copyright: © 2025 by the authors. Licensee MDPI, Basel, Switzerland. This article is an open access article distributed under the terms and conditions of the Creative Commons Attribution (CC BY) license (https://creativecommons.org/licenses/by/4.0/).

1. Introduction

Haploinsufficiency of the *SYNGAP1* gene, most commonly due to loss-of-function single nucleotide variants (SNVs), causes the syndromic neurodevelopmental disorder, *SYNGAP1*-related disorder (SRD). As of October 2024, 1497 individuals have been diagnosed with SRD worldwide [1]. This number has steadily increased over the preceding five years. As late as 2018, only 200 individuals have been diagnosed with SRD [2]. *SYN-GAP1* mutations result in a neurodevelopmental disorder with a phenotype that includes intellectual disability, delayed and impaired motor development, and a high prevalence of epilepsy [3]. Approximately 50% of SRD patients are diagnosed with autism [4,5]. Other abnormal features often include high pain tolerance, hyper-irritability, sleeping difficulties, and a lack of both receptive and expressive language [6,7]. Proper *SYNGAP1* gene dosage is

essential for healthy synaptic development, neuronal function, and plasticity, as determined in both rodent- and human-induced neurons [8,9].

Previous research has documented that between 50 and 70% of individuals with SRD have significant gait abnormalities, with many demonstrating ataxic gait features [4,5,7]. Many SRD patients also experience truncal hypotonia which is likely a key contributor to poor gait as well as overall deficient motor planning, control, and coordination [5]. It has also been reported that individuals may have cerebellar dysfunction [3] and generalized hypotonia, both of which can contribute to disordered gait [7]. Fortunately, there is extensive research being devoted to gene-specific *SYNGAP1*-related disorders that suggests the potential for the development of significant breakthroughs in patient treatment [10,11]. Creson et al., (2019) [12] have demonstrated genetic reversal in mice and there are current trials exploring the use of repurposed drugs for those with SRD [13]. These emerging therapies indicate the need for accurate, reliable, and objective measures for assessment in response to interventions as well as the monitoring of natural behavioral progression over time.

The prevalence of gait problems in the SRD population is a factor in the reduced health and overall quality of life experienced by these patients [14]. To date very little research has been conducted using technology-based techniques to quantitatively assess the gait of individuals with SRD [15]. This paucity leaves a knowledge gap in the identification of the features most prevalent in SRD gait. Using state-of-the-art gait assessment technologies is crucial if a holistic understanding of SRD gait is to be achieved and used for monitoring of natural syndrome phenotype progression and therapeutic response.

Gait features have been explored in this study through a variety of linear and non-linear measures. Temporal measures such as step and stride times are often reported in gait studies [16,17]. Discrete linear measures, such as lower-limb peak angular position and/or velocity, and joint angle range of motions (ROM) are frequently reported. Oftentimes, these variables are used to compute symmetry indices to assess the similarity in these measures between the two legs [18]. Time-series angular waveform assessment included Pearson r correlations between conditions of a single joint, and was used to assess the similarity of the shape of the two waveforms without regard to joint angle amplitude.

In addition to the above measures, the non-linear measures of angle–angle diagrams (A-A) and phase portraits (P-P) were used to identify gait feature differences between SRD and neurotypical individuals. A-A diagrams represent intersegmental coordination by using x-y plots of temporally synchronized time-series waveforms to identify the relative motion of two joints throughout a gait cycle [19,20]. P-Ps use x-y plots of a joint's angular position versus its velocity to explore the control of a particular joint [21,22]. Both types of diagrams can be quantified by calculating the area encompassed by the diagrams to provide additional information about gait dynamics.

The use of linear and non-linear gait measures can identify subtle changes in gait features in response to interventions or over time that would otherwise not be detected using just one or the other. The complementary use of both techniques results in a more comprehensive understanding of the unique mobility challenges of SRD patients and provide insights into specific gait features that can be targeted to improve overall gait performance. Therefore, the primary goal of this study was to employ both linear and non-linear techniques to more fully characterize SRD gait patterns and to quantify the differences between individuals with SRD and neurotypical age-matched participants.

Appl. Sci. 2025, 15, 8267 3 of 15

2. Materials and Methods

2.1. Participants

The participants for this investigation were eight individuals (six females, \overline{X} age = 8.8, SD = 4.8 years) each of which had been diagnosed through clinical evaluations and whole exome sequencing (WES). Participants ranged in age from 4 to 17 years old and were receiving treatment at the Developmental Synaptopathy Clinic at Texas Children's Hospital, in Houston, TX, USA. All were able to walk independently, free of orthotics. None were taking benzodiazepines or any other medication that would be expected to impact their motor control. The study was conducted according to the guidelines of the Declaration of Helsinki and approved by the Institutional Review Board of the Baylor College of Medicine (H-35835) and the University of Houston (00000855). The participants' parents provided written informed consent. Table 1 provides demographic and variant information of each participant.

Table 1. Participant biological sex, age, and genetic mutation.

Participant	Biological Sex	Age	Syngap Genetic Mutation
1	M	9	c.3718C>T (p.R1240X)
2	F	9	c.3190C>T (p.Q1064X)
3	M	8	c.3583-9G>A (IVS16-9G>A)
4	F	12	c.1677-2A>C (IVS10-2A>C)
5	F	4	c.659T>C (p.F220S)
6	F	17	c.3541_3557del (p.K1181Aspfs*3)
7	F	5	c.3535A>T (p.K1179*)
8	F	5	c.3535A>T (p.K1179*)

^{*} stop codon.

2.2. Data Collection

Prior to data collection, infrared reflective markers were placed bilaterally on the anterior and posterior superior iliac crest, mid-lateral femoris (one marker slightly superior to the other), lateral femoral epicondyle, anterolateral mid-shaft of tibia, lateral malleolus, 2nd metatarsophalangeal joint, and calcaneus. This placement was consistent with the recommended Vicon plug-in gait placement and enabled bilateral collection of the hip, knee, and ankle joint motion. All collection procedures were performed by well-trained and experienced doctoral students under the supervision of the two senior authors. The participants then mounted a motorized treadmill (Bertec®, Columbus, OH, USA) and were secured in an overhead harness that prevented falls but did not provide postural support during walking. A static calibration was then obtained. To determine the participants' comfortable walking speed, the task began with the treadmill speed set to 0.1 m/s and was gradually increased by 0.1 m/s until the participants began to display signs of discomfort such as facial and hand motions, or vocalizations, or when the parents indicated the speed should be reduced. The speed was then reduced by 0.2 m/s and was labeled as the participants preferred speed. Once the preferred speed was identified, participants walked for two minutes to acclimate to the treadmill. After a brief rest, data collection was initiated and continued during three minutes of walking. The kinematic data were collected at 100 HZ using a Vicon® 16-camera motion (Vicon, Oxford, UK) capture system and processed with the Nexus v2.15 plug-in gait data processing software. A representation of the data collection environment including the treadmill, harness, and marker placement is displayed in Figure 1.

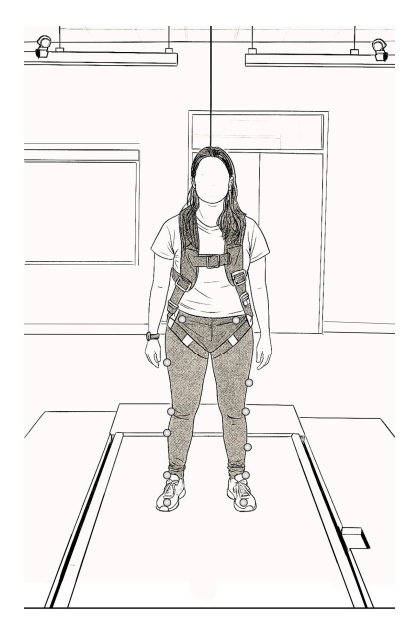


Figure 1. The data collection set up.

2.3. Data Processing

The initial step in data processing involved using a custom Matlab (MathWorks[®]) script to filter the joint angle kinematic data with a 2nd order Butterworth low-pass filter with a 6 Hz cutoff frequency. Due to the fact that heel strike did not occur during a significant number of steps (i.e., toe-walking), the sagittal plane angle waveforms for each joint were partitioned into individual strides using the sample that reflected peak knee flexion [23]. Stride times were then determined based on the number of samples per stride when accounting for sample rate. The filtered waveforms were temporally normalized so that each stride and joint was represented by 100 samples. The mean waveforms for each joint and participant were then calculated.

The data for the neurotypical participants was obtained from a publicly available data set [24]. The authors stated that "This normative data can be used for comparison of pathological gait, thereby improving the interpretation of pathological gait and finally contributing to better clinical decision making (p. 3)." Participants ranged in age from 3 to 17 years old, with multiple participants in each age group. A preferred walking speed was identified prior to data collection. Data was collected in three conditions, in which participants were instructed to walk at their (1) preferred speed, (2) a fast speed (30% greater than preferred), and a slow speed (30% less than preferred). This data set was collected and processed using procedures very similar to those described above, including being collected with the Vicon[®] camera-based motion analysis system, motorized treadmill walking, and data processing using Matlab® R2023b. The raw data was filtered and the joint angle data separated into individual strides and then temporally normalized to 100 samples. For each participant, the average bilateral joint angles for the hip, knee, and ankle were reported. For this study, the data collected at the slow speed was used for comparison as the stride times matched those of our SRD participants. To develop the neurotypical data set, joint angles from participants of the same age as the SRD participants were randomly selected from the published data. For example, for each nine-year-old in the SRD data set, the data from a nine-year-old in the neurotypical data set was randomly selected to contribute to the neurotypical data set. This process resulted in age-matched data sets. Each joint time-series waveform for each participant (neurotypical and SRD) was demeaned by subtracting each individual waveform's mean value from each sample in the

Appl. Sci. **2025**, 15, 8267 5 of 15

waveform. This served to reduce the between-participant variability of the waveforms. All variables described below were computed using custom Matlab (MathWorks[®]) scripts.

2.4. Linear Measures

In addition to stride times, two other linear measures were calculated for each stride and joint: ROM and peak angular velocity. ROM was obtained by first determining the maximum and minimum angular value a joint moved through during a stride. The difference between the two values constituted the ROM. Mean ROM and peak velocity values, plus one SD, were computed for each joint of each participant. Coefficients of variation (CV) represented as a percentage were computed for ROM and peak velocity measures. Symmetry indices (SI) for the peak velocity and ROM data were developed using the formula as follows:

Symmetry index =
$$SI = \frac{|X_G - X_L|}{0.5 \cdot (X_G + X_L)} \cdot 100\%$$

where X_G equals the greater value of the metric and X_L equals the lesser value of the metric. A SI of 0 reflects perfect symmetry between the two limbs [25].

Confidence intervals (CI) at the 95% level, bracketing the neurotypical joint time-series waveforms, were developed and the percentage of SRD waveforms samples that fell outside the CI were obtained [23,26]. Pearson correlation coefficients assessing waveform similarity were developed between each joint's SRD and NT waveform.

2.5. Non-Linear Measures

Using the individual mean waveforms for each joint and participant, angle–angle diagrams and phase portraits were developed. Angle–angle diagrams included the joint pairs hip vs. knee and knee vs. ankle of each leg. Phase portraits for the hip, knee, and ankle for each leg were generated. The area of the diagrams and portraits were then calculated and means and SDs computed. CVs were computed for the angle–angle and phase portraits. Welch's *t*-tests were used to determine if there were differences in the variables between the left and right legs, except for the SIs, as that variable is calculated using the data from both limbs. As there was no difference in any of the variables for either data set, the data were collapsed over the two legs, creating data sets of 16 samples for each variable of both the SRD and neurotypical data sets. Welch's *t*-tests were then used to determine if significant differences existed between the two groups. When appropriate, Bonferroni corrections were applied. To assess the potential difference in the relative variability of the measures between the two groups, the percentage difference in the CVs were calculated for the ROMs, peak velocities, A-A, and P-P areas.

3. Results

3.1. Linear Measures

A Welch's *t*-test showed that there was not a significant difference in stride times between the SRD (\overline{X} = 1.07, SD = 0.19 and neurotypical group \overline{X} = 1.06, SD = 0.15), t(16) = 0.30, p = 0.768.

Table 2 indicates that the mean stride times between the two groups were not different. The peak velocities of the hip and knee of the SRD group were significantly less than those of the NT group, while there was no difference between the ankle velocities of the groups. Although the stride time CV does not reflect a noteworthy difference, the CVs for the peak velocities differ substantially. In all cases the CVs of the SRD group were greater than those of the NT group.

	SRD	NT	p Value	NT CI	
Stride Time	1.07 (0.19)	1.06 (0.16)	0.7680	0.93-1.19	
CV	17.8	15.1			
Peak Velocity	SRD	NT		NT CI	
Hip	1.43 (0.23) *	2.21 (0.24)	0.0001	2.01-2.41	
CV	16.1	10.9			
Knee	2.20 (0.31) *	3.75 (0.21)	0.0001	3.57-3.93	
CV	14.1	5.6			
Ankle	1.30 (0.59)	1.21 (0.30)	0.6547	0.96–1.46	
CV	45.4	24.8			

Table 2. Mean and SD stride times, peak joint velocities, CVs, and CIs of NT participants.

Table 3 shows that the ROM of the hip and knee of the SRD group is significantly less than that of the NT group. Although trending in the same direction as the other joints, the SRD ankle is not significantly different than NT ROM, with the substantial variability of the SRD group likely accounting for the lack of significance. The CVs for all joints indicate that the relative variability of SRD participants is substantially greater than that of the NT participants.

Table 3. Mean ROMs and SDs, CVs, and CI of NT participants.

ROM	SRD	NT	p Value	NT CI
Hip	26.4 (6.3) *	42.1 (5.0)	0.0001	37.9–46.3
CV	23.8	11.9		
Knee	33.9 (7.7) *	63.30 (5.7)	0.0001	58.5–68.1
CV	22.3	9.0		
Ankle	18.3 (10.5)	24.3 (4.7)	0.3054	20.4–28.2
CV	57.4	19.3		

^{*} represents statistical difference between SRD and NT, with a Bonferroni corrected alpha level of 0.0167.

Figure 2 reflects that the basic mean movement pattern is fairly similar between the two groups but the amplitude of the SRD waveform across the stride is different for each joint (see also Tables 3 and 4).

Table 4 presents the mean and SD SI values for the ROMs and peak joint velocities of each joint for both groups. These data reflect that the asymmetry between the two limbs, for both measures, is much greater in the SRD participants than the NT participants as all of the SRD values fall outside of the NT CI bounds.

Table 5 represents that for each joint, the waveforms of the SRD group display a high degree of similarity with those of the NT group, but the vast majority of the SRD samples falls outside the CIs of the NT waveforms.

^{*} represents statistical difference between SRD and NT, with a Bonferroni corrected alpha level of 0.0167.

Appl. Sci. 2025, 15, 8267 7 of 15

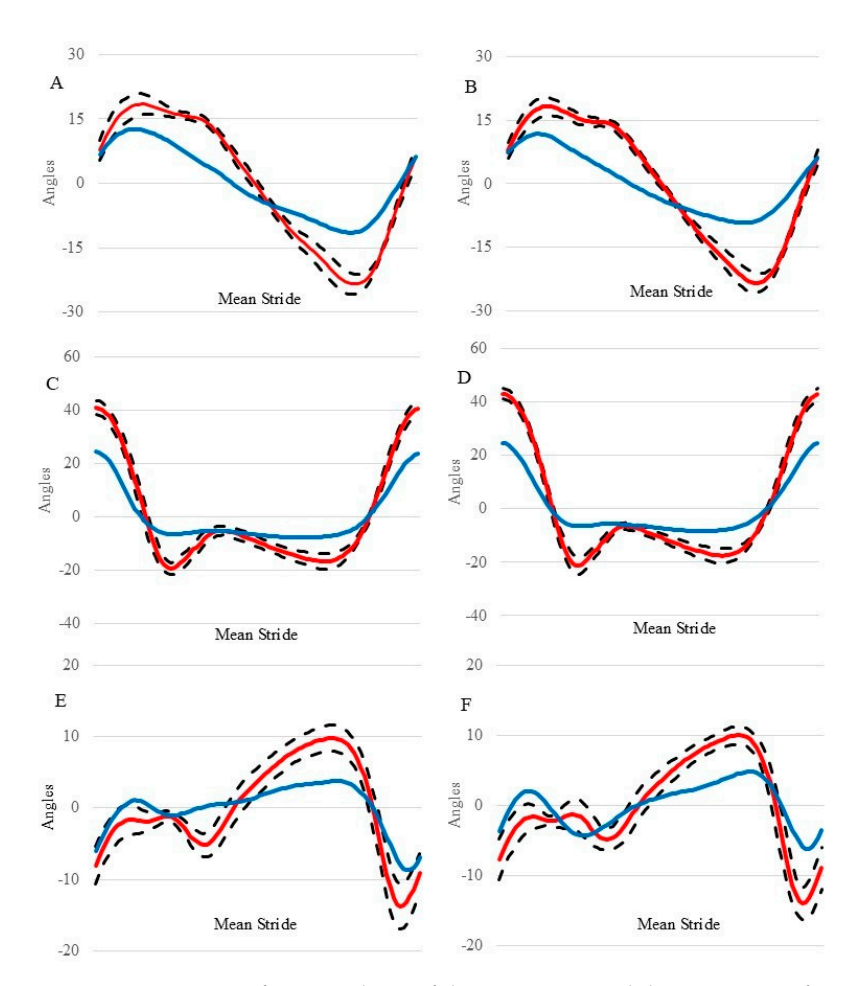


Figure 2. Mean waveforms and CIs of the NT group and the mean waveform of the SRD group for each joint. The blue waveforms represent the SRD group, red waveforms represent the NT, and the dash lines represent the 95% CI for the NT group. Panels (**A,C,E**) are from the left leg and (**B,D,F**) are from the right leg. Top panels represent Hip, middle panels represent Knee and bottom panels represent Ankle. Values above 0 degrees represent flexion, while values below 0 represent extension.

Table 4. Mean SI and SD for each joint of the SRD and NT groups.

ROM	HIP		Kn	Knee		Ankle	
SI	-20.2 (14.1)	-10.0 (8.8)	-43.3 (48.9)	-12.1 (7.9)	-138.8 (77.1)	-27.2 (18.8)	
CI	-17.52.8		-18.65.7		-42.811.7		
Velocity (deg/s)							
SI	-21.6 (11.7)	12.0 (7.8)	-39.0 (42.0)	-8.8 (7.5)	-117.5 (94.8)	-26.7 (28.2)	
CI	-18.45.5		-14.82.7		-50.33.1		

SRD—left columns, NT—right columns, CIs of NT group.

Table 5. Pearson r correlation values and the percentage of SRD samples outside the NT CIs for each joint, between the waveforms of SRD and NT groups. All correlation values exceeded the critical r-value of 0.798, corresponding to an alpha level of 0.005.

	L Hip	L Knee	L Ankle	R Hip	R Knee	R Ankle
Pearson r values	0.96	0.98	0.92	0.91	0.98	0.88
Percentage	92%	84%	83%	94%	91%	80%

3.2. Non-Linear Measures

Figure 3 displays the NT and SRD mean hip–knee and knee–ankle angle–angle figures. While the shape of the waveforms is very similar between the two groups, the amplitude of the SRD is significantly smaller than that of the NT waveform.

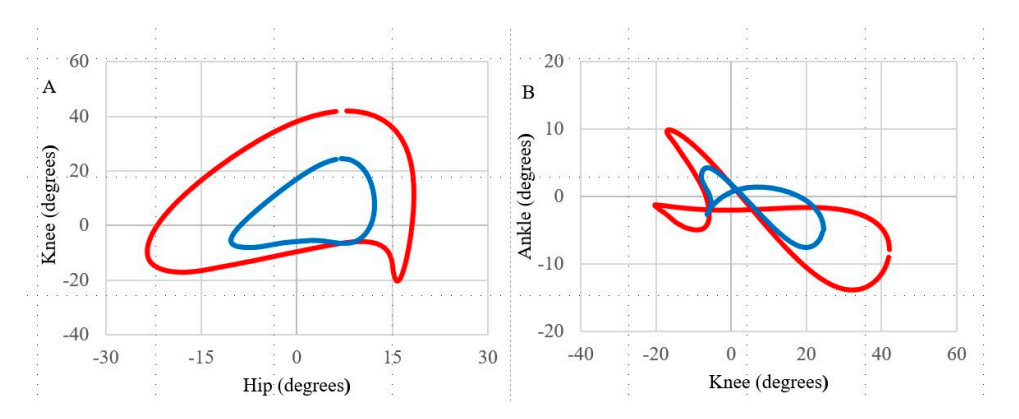


Figure 3. Angle–angle hip versus knee (**A**), and knee versus ankle (**B**) waveforms of the SRD and NT groups. Blue represents the SRD participants and red represents the NT participants. Positive values represent flexion while negative values represent extension.

Table 6 shows that the two angle–angle area comparisons were significantly different between the two groups. Table 7 indicates the phase portrait areas of the hip and knee were significantly different while the ankle comparison failed to reach significance using the Bonferroni alpha correction. In all cases, the SRD group has smaller values than that of the NT group. Also note that there are substantial differences in the relative variability (i.e., CVs).

Table 6. Angle–angle and phase portrait mean areas and SDs, for the SRD and NT groups.

		SRD Hip vs. Knee	NT Hip vs. Knee	p Value	SRD Knee vs. Ankle	NT Knee vs. Ankle	p Value
Angle–angle areas (mm ²)	Mean SD	582 * 222	1689 316	0.0001	214 * 110	426 85	0.0001

^{*} represents statistical difference between SRD and NT, with a Bonferroni correct alpha level of 0.025.

Table 7. Phase portrait mean areas and SDs, for the SRD and NT groups.

		SRD Hip	NT Hip	p Value
Phase portrait areas (deg2/% of gait cycle)	Mean (SD)	40 * (14)	106 (22)	0.0001
	CV	34.5	21.1	
Phase portrait areas (deg2/% of gait cycle)	Mean (SD)	114 * (42)	403 (71)	0.0001
	CV	36.8	17.6	
Phase portrait areas (deg2/% of gait cycle)	Mean SD	42 (39)	67 (18)	0.0331
	CV	92.9	26.0	

^{*} represents statistical difference between SRD and NT, with a Bonferroni correct alpha level of 0.0167.

Figure 4 displays the mean phase portraits of the two groups for the hip, knee, and ankle. Similarly to the angle–angle figures, the shape of the portraits was comparable between the two groups and the SRD waveforms were significantly smaller than those of the NT group.

Appl. Sci. 2025, 15, 8267 9 of 15

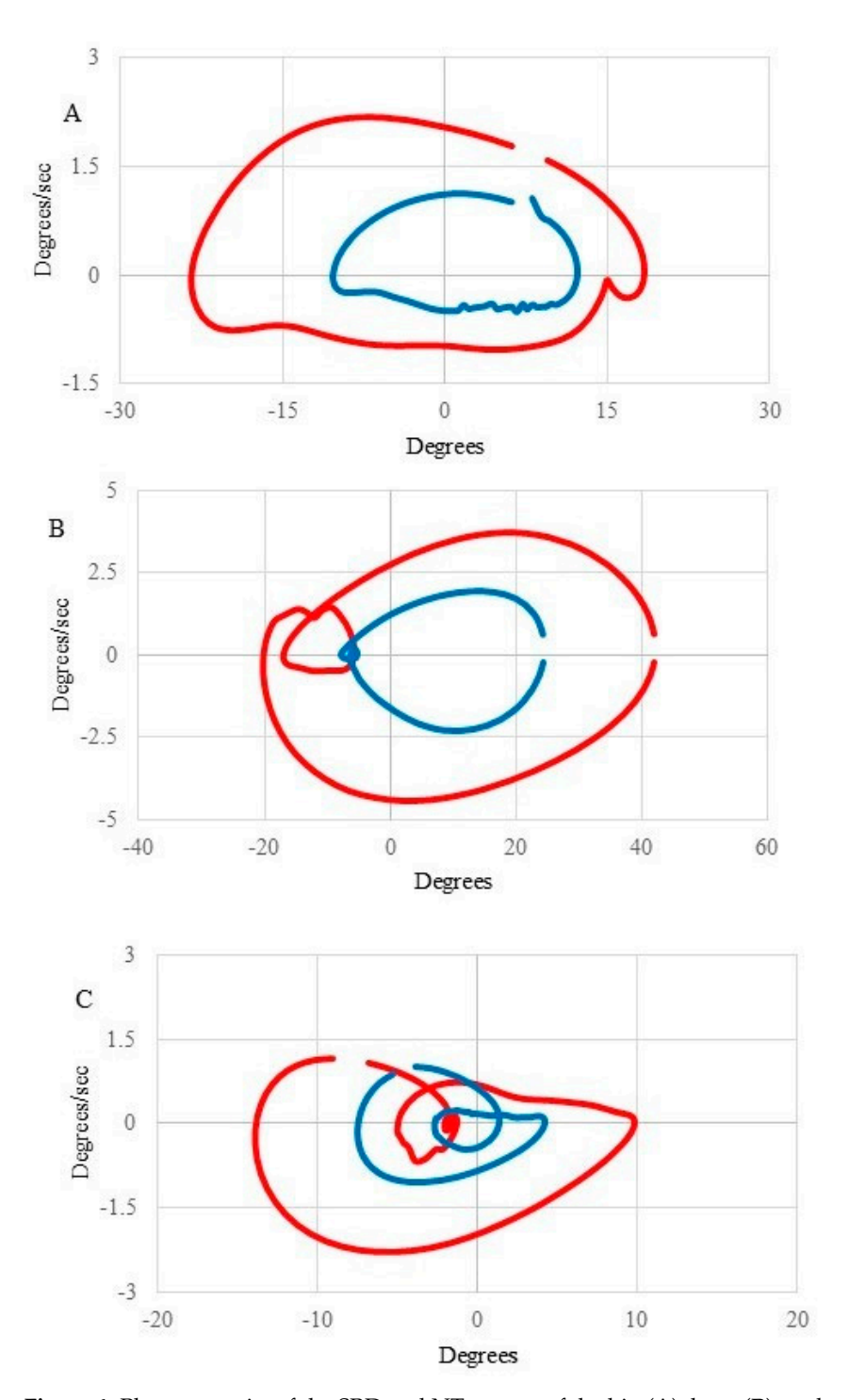


Figure 4. Phase portraits of the SRD and NT groups of the hip (A), knee (B), and ankle (C).

Blue represents the SRD participants and red represents the NT participants. Positive values represent flexion and negative values represent extension.

Table 8 displays the CVs and percentage differences between the groups for the various measures. The data indicate that the SRD group had much greater relative variability than the NT group, as reflected in the large percentage differences.

Table 8. CVs of SRD and NT groups of ROMs, peak velocities, A-A, and P-P areas
--

CVs		Hip	Knee	Ankle		
ROM	SRD	23.8	22.3	57.4		
110111	NT	11.9	9.0	19.3		
	% Delta	100	148	197		
Peak Velocity	SRD	16.1	14.1	45.4		
	NT	10.9	5.6	24.8		
	% Delta	48	152	83		
		Hip v	s. Knee	Knee	vs. Ankle	
A-A Area	SRD	38.2			51.1	
71 71 71 Cu	NT	18.7			20.0	
	% Delta	104			156	
		Hip]	Knee	Ankle
P-P Area	SRD	65.5			70.3	174.3
1 1 11100	NT	4	0.0		33.2	51.5
	% Delta	(58		156	214

4. Discussion

Gait quality has been shown to closely correlate with overall health status in neurotypical individuals [27]. In individuals with neurodevelopmental disorders, gait quality is associated with the severity of their condition, suggesting that comprehensive gait assessment may possibly offer valuable insights into their overall health status [14,28]. Much of the existing literature describing the motoric characteristics of individuals with SRD have come from observational surveys, primarily focused on fundamental motor skills and fine motor skills related to activities of daily living. More formal surveys have included the use of the Alberta Infant Motor Scale, various subtests of the Bayley Scale of Infant and Toddler Development, and the Gross Motor Function Measure (GMFM).

Gait quality is increasingly being considered as a possible non-invasive biomarker [29]. Therefore, it is important that gait metrics of individuals with SRD are accurately measured quantitatively and objectively using state-of-the art motion analysis technologies and analyzed with a variety of techniques. To explore the possibility that gait could serve as a biomarker, more laboratory-based studies with significant numbers of participants need to be conducted. However, as mentioned previously, the only laboratory-based evaluation of gait with SRD participants was conducted by [15], and this study had limited generalizability as only one individual with SRD participated. Expansion of the number of SRD gait studies as well as increased numbers of participants are needed before meaningful examination of potential relationships between clinically accepted motor scales and gait measures can be conducted. The current report characterizes the gait of eight participants with SRD and compares the outcomes to those of age-matched controls, thereby representing a significant increase in the number of participants compared to the previous report from our group.

As there are no differences in stride times between the two groups (Table 2), potential changes in the additional gait measures can be interpreted as results from differences in coordination or control, and not temporal features of the stride. The SDs for the two groups also indicate that stride time variability is very similar for the two groups. As the SRD and NT groups are composed of age-matched participants, the stride time data suggests that

individuals with SRD are quite capable of producing gait cadence that match the slow speed of NT individuals, at least during motorized-driven treadmill walking. The rhythmical pattern of lower-limb motion is proposed to be generated by a complex of spinal neurons requiring the intervention of higher-order structures to produce functional walking [30,31]. This spinal complex is labeled as a central pattern generator, more commonly known as a CPG. The matching stride times of the two groups may indicate that the CPG complex remains functionally intact in those with SRD. However, as the results indicate, there are substantial differences between the gait metrics of individuals with SRD and age-matched neurotypical controls, particularly with regard to the magnitude and variability of joint motion. This suggests that other physiological mechanisms are likely contributing to the dysfunctional gait of individuals with SRD. As mentioned in the introduction, hypotonia, particularly truncal hypotonia, cerebellar deficits, muscle weakness, and dyspraxia all likely play a role in the disordered gait [3,5,7,32].

Table 2 reflects that despite no differences in stride times, the peak velocity of the hip and knee of the SRD participants is significantly less than the NT participants. However, there is no difference in the ankle peak velocity. Similarly to Table 2, Table 3 shows that the SRD ROMs of the hip and knee are also less than the NT group, with no difference at the ankle. Peak velocities and ROMs are discrete measures that provide useful summary 'snapshots' of joint behavior but convey no information about how a joint is moving through space over the course of a stride. However, when discrete measures are combined with nonlinear measures, a more complete representation of a joint's behavior is revealed. Enhanced representation can provide greater insights into time periods when gait patterns between two groups differ and how the joints move through space individually and relative to each other.

Figure 1 illustrates the above idea. It can be observed that the 'shape' (i.e., when the joint is moving in flexion or extension) is similar between the two groups for a given joint. This visualization is confirmed by the high correlations reported in Table 5. However, despite the similarity in the shape, it is obvious that the amplitudes of the waveforms differ between the SRD and NT participants. This is confirmed by the high percentage of the SRD samples that fall outside the 95% CIs of the NT group, for all joints. Further, by evaluating the entire waveform, and using the NT waveform as the reference, we find that at times, the SRD waveforms exhibit greater flexion/extension while at other times the SRD waveforms exhibit less flexion/extension. This information is not readily available if only the discrete ROM value is calculated.

To execute effective goal-directed gait, intra-segmental coordination must be achieved. While the waveforms in Figure 1 are informative, they provide little information about how the joints within a given leg are coordinated, or how joints across the two legs work together. A-A diagrams provide such information. Consistent with the reduced ROMs of the SRD group for all joints, the areas of the hip-vs-knee and knee-vs-ankle are significantly less than those of the NT group, as reported in Table 6. Not surprisingly, however, is the similar shape of the A-A diagrams between the two groups. This is to be expected given the time-series waveforms also have similar shapes. Figure 2 reveals that the reduction in the ROM for the SRD group's waveforms occurs throughout the stride, for each joint, resulting in considerably compressed waveforms, and consequently, significantly reduced areas. Therefore, although the coordination pattern between the joints is very similar, the SRD group's joints are moving through significantly smaller regions of space compared to the NT groups.

Although information about the motion of the joint through space across the stride is available in Figure 1, information about the velocity at which the joints move through space is absent. The peak velocities listed in Table 2 indicate that there are differences

between the groups for the two proximal joints. These discrete peak velocity differences suggest that the control of the joints is different between the two groups. However, with a time-series graph, it is impossible to determine where velocities are similar and where they are different across the stride. However, this information can be determined through visual inspection of phase-portraits. Figure 4 reveals that the velocity of all the measured joints for the SRD participants is reduced throughout the entire stride and again resulting in smaller P-P areas relative to the NT participants. As P-Ps reflect joint control features, Figure 4 and Table 7 confirm a significant difference in lower-limb control between the two groups throughout the stride that cannot be discerned from observing peak velocity values alone. This is especially true for the ankle, where the areas of the ankle P-P reflect a significant difference, but no difference in the peak velocities (Figure 4 and Table 2).

In addition to the necessity of intra-segmental coordination, inter-limb coordination is also necessary for effective walking. SIs are a common technique to assess inter-limb coordination by comparing the degree of equality of the behavior between joints of the two legs. Table 4 reflects large differences in the SIs for the ROM for all joints, with the SRD group being less symmetrical than the NT group. Likewise, the symmetry between the legs for each joint is less in the SRD participants than the NT participants. In all cases, the variability (i.e., SD) is much greater in the SRD compared to the NT group for both the ROM and peak velocities. The only exception is the hip peak velocity SDs. In combination, these measures reflect the increased difficulty of the SRD participants to finely coordinate and control their two limbs to produce symmetrical walking patterns. Given that the treadmill belt was moving at a fixed speed, and there were still difficulties in producing symmetrical gait, it is expected that further decreases in symmetry occur during overground walking.

It should also be noted that the CVs of the SRD group for all measures are much greater, reflecting more relative variability in this group compared to the NT group. For both groups the relative variability of the ankle always exceeds that of the hip and knee. This indicates that across the sample, both groups displayed a wider range of ankle joint behaviors, in terms of both joint angular position and velocity, than the two more proximal joints. Although the pattern of variability across the joints is the same between the two groups, the magnitude of relative variability is much greater in the SRD group. Table 8 displays CV comparisons between the two groups, with eight of those revealing the SRD values were 100 or more percent greater than those of the NT group. This also indicates a wider range of joint behaviors, for all joints, exhibited by the SRD group.

The amount of relative variability is not a function of the age of the participants, as the NT group always displayed less than the SRD group despite each participant being aged-matched with a participant from the other group. This suggests that there is not a stereotypical gait pattern that can be labeled as 'SRD gait', in the sense that stereotypical gait patterns of individuals with Parkinson's disease produce 'Parkinsonian gait'. These findings also indicate that individuals with SRD are more likely to produce individualized gait patterns regardless of age. This contrasts with NT participants who from a very young age produce very a stereotypical gait pattern that is often labeled as 'healthy gait'.

Overall, the patterns of differences between the SRD and NT groups are consistent with the findings of the Layne et al., (2022) report [15] which used some of the same analysis techniques as the current report. However, those authors discussed a single case study of one individual with SRD whose gait measures were compared to that of a single age-matched NT individual. The current study expands on that previous work through a significant increase in the number of participants and a measure of intra-segmental coordination (i.e., A-A areas). Like the previous work, the use of both linear and non-linear measures allows for a greater characterization of gait patterns than using a single category of measures. Documenting how joint behavior changes throughout the gait cycle provides

clinicians and investigators with important information about underlying neuromuscular features that need to be modified to produce more efficient gait. Potential subtle changes in gait, be they the results of therapeutic intervention or developmental regression, can be more easily detected with a variety of analysis techniques compared to being observable to the human eye.

Limitations and Future Work

Although greatly increasing the number of individuals with SRD compared to Layne et al., (2022) [15], the total of eight participants in this study remains far short of the number required to more fully characterize the range of gait patterns associated with the SRD gait. This relatively low number of participants does limit the ability to generalize the findings but does substantially increase the number of participants with SRD who have participated in a laboratory-based study of gait. The current report does provide the first laboratory-based quantitative measures of gait variability in the SRD population. The limited number of participants does prevent answering the question of whether age is associated with either progression or regression of gait in SRD. Thus, future work should continue to expand the number of individuals with SRD participating in laboratory-based gait investigations across all age groups. Additionally, comparisons of gait performance between SRD patients and individuals with other genetic disorders, such as Rett Syndrome, would provide useful information to researchers and clinicians. The application of a variety of linear and non-linear techniques should also be used to characterize overground walking of individuals with SRD, with comparisons made to gait characteristics obtained during treadmill walking. Although treadmill walking offers the advantage of a more controlled environment that allows for the study of the basic gait pattern, fall prevention harnesses offer a degree of protection that is typically not available during overground walking. Therefore, the need for greater dynamic postural control is increased during overground walking, relative to treadmill walking. As overground walking is the 'natural' form of locomotion, with its emphasis on goal-directed behavior, overground walking presents the opportunity to adapt to the environment. However, that very opportunity also creates circumstances that allow extremely variable gait patterns, including stopping, turning, and completely walking off electronic gait mats that are often used to collect data during overground walking. These behaviors result in modified segmental gait motions and associated metrics when compared to the less variable treadmill-driven gait motions. A future manuscript will explore the potential differences between treadmill and overground gaits.

Advances in computing power have resulted in the development of powerful analytical techniques that can lead to insights that were previously difficult to uncover. In particular, machine learning approaches have opened new vistas in the understanding of gait control of both neurotypical and patient populations [33]. Identifying relevant gait features by reducing dimensionality and classification, as well as clustering techniques, are just a few of the ways that machine learning has assisted in identifying clinical gait patterns and diagnoses. For a recent review see Dibbern et al., 2025 [33]. Recently, the use of machine learning has been proposed to create a 'healthy' digital twin for individuals with a disordered gait that provides individualized predictions of joint kinematics during the gait cycle. This procedure serves to help identify stride kinematics that emulate neurotypical patterns versus disordered stride kinematics [34]. The above are just a few of the ways machine learning can be useful to investigators and clinicians attempting to characterize, understand, diagnose, and ultimately improve the gait performance of a variety of populations. As kinematic data sets expand in both the number of participants and number of

strides, machine learning is expected to play an ever-increasing role in the analysis of gait patterns produced by individuals with SRD.

Author Contributions: C.S.L.: conceptualization, investigation and methodology, writing—original draft, visualization; D.M.D.: investigation and methodology, writing—review and editing; C.A.M.: investigation and methodology, writing—review and editing; B.S.: conceptualization, writing—review and editing, J.L.H.J.:—conceptualization, interpreted the data and edited the manuscript. All authors have read and agreed to the published version of the manuscript.

Funding: This study was funded by the SYNGAP1 Foundation with a grant to J.L.H.J.

Institutional Review Board Statement: This study was conducted in accordance with the Declaration of Helsinki and approved by the Institutional Review Boards at the Baylor College of Medicine (H-35835) and University of Houston and the University of Houston (00000855).

Informed Consent Statement: The participants' parents provided written informed consent.

Data Availability Statement: The raw data supporting the conclusions of this article will be made available by the authors on request.

Acknowledgments: We are greatly appreciative of all of our participants, their parents, and caregivers who, without their willingness to volunteer, this study would not have been possible.

Conflicts of Interest: The authors declare no conflicts of interest.

References

- 1. SynGAP Research Fund. SYNGAP1 CENSUS 2024 Update. Retrieved from SYNGAP1 CENSUS 2024 Update: +43 in Q3 2024; Total = 1497—Syngap Research Fund. 2024. Available online: https://curesyngap1.org/blog/syngap1-census-2024-update-43-in-q3-2024-total-1497/ (accessed on 19 May 2025).
- 2. Weldon, M.; Kilinc, M.; Lloyd Holder, J.; Rumbaugh, G. The first international conference on *SYNGAP1*-related brain disorders: A stakeholder meeting of families, researchers, clinicians, and regulators. *J. Neurodev. Disord.* **2018**, *10*, 6. [CrossRef] [PubMed]
- 3. Agarwal, M.; Johnston, M.V.; Stafstrom, C.E. *SYNGAP1* mutations: Clinical, genetic, and pathophysiological features. *Int. J. Dev. Neurosci.* **2019**, *78*, 65–76. [CrossRef] [PubMed]
- 4. Mignot, C.; von Stülpnagel, C.; Nava, C.; Ville, D.; Sanlaville, D.; Lesca, G.; Rastetter, A.; Gachet, B.; Marie, Y.; Korenke, G.C.; et al. Genetic and neurodevelopmental spectrum of *SYNGAP1* -associated intellectual disability and epilepsy. *J. Med. Genet.* **2016**, *53*, 511–522. [CrossRef] [PubMed]
- 5. Parker, M.J.; Fryer, A.E.; Shears, D.J.; Lachlan, K.L.; McKee, S.A.; Magee, A.C.; Mohammed, S.; Vasudevan, P.C.; Park, S.-M.; Benoit, V.; et al. De novo, heterozygous, loss-of-function mutations in *SYNGAP1* cause a syndromic form of intellectual disability: *SYNGAP1* Syndrome. *Am. J. Med. Genet.* 2015, 167, 2231–2237. [CrossRef] [PubMed]
- 6. Holder, J.L.; Hamdan, F.F.; Michaud, J.L. SYNGAP1-Related Intellectual Disability. In *GeneReviews*®; Adam, M.P., Feldman, J., Mirzaa, G.M., Pagon, R.A., Wallace, S.E., Amemiya, A., Eds.; University of Washington: Seattle, WA, USA, 2019.
- 7. Vlaskamp, D.R.M.; Shaw, B.J.; Burgess, R.; Mei, D.; Montomoli, M.; Xie, H.; Myers, C.T.; Bennett, M.F.; XiangWei, W.; Williams, D.; et al. *SYNGAP1* encephalopathy: A distinctive generalized developmental and epileptic encephalopathy. *Neurology* **2019**, 92, e96–e107. [CrossRef] [PubMed]
- 8. Araki, Y.; Gerber, E.E.; Rajkovich, K.E.; Hong, I.; Johnson, R.C.; Lee, H.K.; Kirkwood, A.; Huganir, R.L. Mouse models of *SYNGAP1*-related intellectual disability. *Proc. Natl. Acad. Sci. USA* **2023**, *120*, e2308891120. [CrossRef] [PubMed]
- 9. Llamosas, N.; Arora, V.; Vij, R.; Kilinc, M.; Bijoch, L.; Rojas, C.; Reich, A.; Sridharan, B.; Willems, E.; Piper, D.R.; et al. *SYNGAP1* Controls the Maturation of Dendrites, Synaptic Function, and Network Activity in Developing Human Neurons. *J. Neurosci.* **2020**, 7980–7994. [CrossRef] [PubMed]
- 10. John Hopkins University Technology Publisher. *Available Technologies*; John Hopkins University Technology Publisher: Baltimore, MD, USA, 2024.
- 11. Yang, R.; Feng, X.; Arias-Cavieres, A.; Mitchell, R.M.; Polo, A.; Hu, K.; Zhong, R.; Qi, C.; Zhang, R.S.; Westneat, N.; et al. Upregulation of *SYNGAP1* expression in mice and human neurons by redirecting alternative splicing. *Neuron* **2023**, *111*, 1637–1650.e5. [CrossRef] [PubMed]
- 12. Creson, T.K.; Rojas, C.; Hwaun, E.; Vaissiere, T.; Kilinc, M.; Jimenez-Gomez, A.; Holder, J.L., Jr.; Tang, J.; Colgin, L.L.; Miller, C.A.; et al. Re-expression of SynGAP protein in adulthood improves translatable measures of brain function and behavior. *eLife* **2019**, 8, e46752. [CrossRef] [PubMed]

13. Graglia, J.M.; Harding, A.J.; Helde, K.A. Roadmap to advance therapeutics for *SYNGAP1*-related disorder: A patient organization perspective from SynGAP Research Fund. *Ther. Adv. Rare. Dis.* **2025**, *6*, 26330040241308285. [CrossRef] [PubMed]

- 14. Bolbocean, C.; Andújar, F.N.; McCormack, M.; Suter, B.; Holder, J.L., Jr. Health-related quality of life in pediatric patients with syndromic autism and their caregivers. *J. Autism Dev. Disord.* **2022**, *52*, 1334–1345. [CrossRef] [PubMed]
- 15. Layne, C.S.; Malaya, C.A.; Young, D.R.; Suter, B.; Holder, J.L., Jr. Comparison of treadmill gait between a pediatric-aged individual with *SYNGAP1*-related intellectual disability and a fraternal twin. *Front. Hum. Neurosci.* **2022**, *16*, 918918. [CrossRef] [PubMed]
- 16. Bates, A.V.; McGregor, A.H.; Alexander, C.M. Comparing sagittal plane kinematics and kinetics of gait and stair climbing between hypermobile and non-hypermobile people; a cross-sectional study. *BMC Musculoskelet*. *Disord*. **2021**, 22, 712. [CrossRef] [PubMed]
- 17. van Bloemendaal, M.; Beelen, A.; Kleissen, R.F.M.; Geurts, A.C.; Nollet, F.; Bus, S.A. Concurrent validity and reliability of a low-cost gait analysis system for assessment of spatiotemporal gait parameters. *J. Rehabil. Med.* **2019**, *51*, 456–463. [CrossRef] [PubMed]
- 18. Siebers, H.; Alrawashdeh, W.; Betsch, M.; Migliorini, F.; Hildebrand, F.; Eschweiler, J. Comparison of different symmetry indices for the quantification of dynamic joint angles. *BMC Sports Sci. Med. Rehabil.* **2021**, *13*, 130. [CrossRef]
- 19. de Bruin, H.; Russell, D.J.; Latter, J.E.; Sadler, J.T. Angle-angle diagrams in monitoring and quantification of gait patterns for children with cerebral palsy. *Am. J. Phys. Med.* **1982**, *61*, 176–192. [PubMed]
- 20. Winstein, C.J.; Garfinkel, A. Qualitative dynamics of disordered human locomotion: A preliminary investigation. *J. Mot. Behav.* **1989**, 21, 373–391. [CrossRef] [PubMed]
- 21. Hurmuzlu, Y.; Basdogan, C.; Carollo, J.J. Presenting joint kinematics of human locomotion using phase plane portraits and Poincaré maps. *J. Biomech.* **1994**, 27, 1495–1499. [CrossRef] [PubMed]
- 22. Stergiou, N.; Jensen, J.L.; Bates, B.T.; Scholten, S.D.; Tzetzis, G. A dynamical systems investigation of lower extremity coordination during running over obstacles. *Clin. Biomech.* **2001**, *16*, 213–221. [CrossRef] [PubMed]
- 23. Layne, C.S.; Diaz, D.; Malaya, C.; Futrell, B.; Alfaro, C.; Gustafson, H.; Suter, B. Using Linear and Non-Linear Techniques to Characterize Gait Coordination Patterns of Two Individuals with NGLY1 Deficiency. *CRCM* **2024**, *13*, 391–409. [CrossRef]
- 24. Senden, R.; Marcellis, R.; Meijer, K.; Willems, P.; Lenssen, T.; Staal, H.; Janssen, Y.; Groen, V.; Vermeulen, R.J.; Witlox, M. Dataset of 3D gait analysis in typically developing children walking at three different speeds on an instrumented treadmill in virtual reality. *Data Br.* 2023, 48, 109142. [CrossRef] [PubMed]
- 25. Hu, Y.; Zou, D.; Jiang, M.; Qian, Q.; Li, H.; Tsai, T.-Y.; Zhang, J. Postoperative hip center position is associated with gait symmetry in range of axial rotation in dysplasia patients after THA. *Front. Surg.* **2023**, *10*, 1135327. [CrossRef] [PubMed]
- 26. Duhamel, A.; Bourriez, J.L.; Devos, P.; Krystkowiak, P.; Destée, A.; Derambure, P.; Defebvre, L. Statistical tools for clinical gait analysis. *Gait Posture* 2004, 20, 204–212. [CrossRef] [PubMed]
- 27. Rasmussen, L.J.H.; Caspi, A.; Ambler, A.; Broadbent, J.M.; Cohen, H.J.; d'Arbeloff, T.; Elliott, M.; Hancox, R.J.; Harrington, H.; Hogan, S.; et al. Association of neurocognitive and physical function with gait speed in midlife. *JAMA Netw. Open.* 2019, 2, e1913123. [CrossRef] [PubMed]
- 28. Cuddapah, V.A.; Pillai, R.B.; Shekar, K.V.; Lane, J.B.; Motil, K.J.; Skinner, S.A.; Tarquinio, D.C.; Glaze, D.G.; McGwin, G.; Kaufmann, W.E.; et al. Methyl-CpG-binding protein 2 (MECP2) mutation type is associated with disease severity in Rett syndrome. *J. Med. Genet.* 2014, 51, 152–158. [CrossRef] [PubMed]
- Servais, L.; Strijbos, P.; Poleur, M.; Mirea, A.; Butoianu, N.; Sansone, V.A.; Vuillerot, C.; Schara-Schmidt, U.; Scoto, M.; Seferian, A.M.; et al. Evidentiary basis of the first regulatory qualification of a digital primary efficacy endpoint. Sci. Rep. 2024, 14, 29681. [CrossRef] [PubMed]
- 30. Danner, S.M.; Hofstoetter, U.S.; Freundl, B.; Binder, H.; Mayr, W.; Rattay, F.; Minassian, K. Human spinal locomotor control is based on flexibly organized burst generators. *Brain* **2015**, *138*, 577–588. [CrossRef] [PubMed]
- 31. Haghpanah, S.A.; Farahmand, F.; Zohoor, H. Modular neuromuscular control of human locomotion by central pattern generator. *J. Biomech.* **2017**, *53*, 154–162. [CrossRef] [PubMed]
- 32. Wright, D.; Kenny, A.; Eley, S.; McKechanie, A.G.; Stanfield, A.C. Clinical and behavioural features of *SYNGAP1*-related intellectual disability: A parent and caregiver description. *J. Neurodev. Disord.* **2022**, *14*, 34. [CrossRef] [PubMed]
- 33. Dibbern, K.N.; Krzak, M.G.; Olivas, A.; Albert, M.V.; Krzak, J.J.; Kruger, K.M. Scoping Review of Machine Learning Techniques in Marker-Based Clinical Gait Analysis. *Bioengineering* **2025**, *12*, 591. [CrossRef] [PubMed]
- 34. Trusov, P.M.; Diaz, D.M.; Layne, C.S. Digital Twin-Based Controls in Gait Analysis: A Machine Learning Approach. *J. Phys. Med. Rehabil.* **2024**, 12, 27. Available online: https://www.longdom.org/open-access/digital-twinbased-controls-in-gait-analysis-a-machine-learning-approach-1100550.html (accessed on 19 May 2025).

Disclaimer/Publisher's Note: The statements, opinions and data contained in all publications are solely those of the individual author(s) and contributor(s) and not of MDPI and/or the editor(s). MDPI and/or the editor(s) disclaim responsibility for any injury to people or property resulting from any ideas, methods, instructions or products referred to in the content.